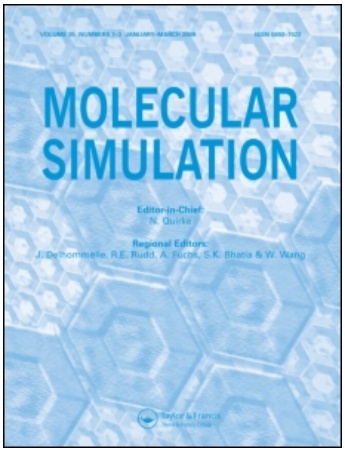

Molecular Simulation
Publication details, including instructions for authors and subscription information:
http://www.informaworld.com/smpp/title~content=t713644482

Transition Path Sampling Study of the Local Molecular Structure in the Aqueous Solvation of Sodium Chloride

J. Martí[ab]
[a] Departament de Física i Enginyeria Nuclear, Universitat Politècnica de Catalunya, Barcelona, Catalonia, Spain, EU [b] Department of Chemistry, University of California, Berkeley, CA, USA

To cite this Article Martí, J.(2001) 'Transition Path Sampling Study of the Local Molecular Structure in the Aqueous Solvation of Sodium Chloride', Molecular Simulation, 27: 3, 169 — 185
To link to this Article: DOI: 10.1080/08927020108023022
URL: http://dx.doi.org/10.1080/08927020108023022

Molecular Simulation, 2001, Vol. 27, pp. 169–185
Reprints available directly from the publisher
Photocopying permitted by license only

TRANSITION PATH SAMPLING STUDY OF THE LOCAL MOLECULAR STRUCTURE IN THE AQUEOUS SOLVATION OF SODIUM CHLORIDE

J. MARTÍ

Departament de Física i Enginyeria Nuclear, Universitat Politècnica de Catalunya, B5-206 Campus Nord UPC, 08034 Barcelona, Catalonia, Spain, EU and Department of Chemistry, University of California, Berkeley, CA 94720, USA

(Received July 2000; accepted September 2000)

The aqueous solvation of sodium chloride has been investigated using the recently introduced technique of the transition path sampling. We performed a series of Monte Carlo simulations for each element of an ensemble of chains of states. The evolution of the local solvent structure during the dissociation process has been observed. The incoming of a couple of waters to the first coordination shell is responsible for the structural changes which allow the dissociation occur: waters which leave the second coordination shell produce voids and a local molecular reorganization in order to allocate the dissociated ion pair.

Keywords: Monte Carlo simulation; Transition path sampling; Ionic solvation; Local molecular structure

1. INTRODUCTION

The study of rare events in chemical systems has become the subject of many theoretical works along the last decades. Rare events play a central role in a variety of fields like chemical kinetics, diffusion in solids or in the electrical transport theory, to mention a few examples. We can define a *rare event* as a phenomenon which takes place in a time scale much longer than the typical time associated to the microscopic dynamics of the system. The characterization of rare events is deeply concerned with the location of the *transition states* (TS) of the system [1]. In a chemical reaction the system

evolves in time from one stable state to another, visiting one or more TS which can be observed as saddle points located on a rugged potential energy surface. We can sketch the process employing only two spatial coordinates, as it is shown in Figure 1. We can observe how the system evolves from the stable state A to the stable state B through configurational space. During evolution, it crosses the TS. The reader should note that to perform such a transition, the time spent by the system is, in general, much longer than the typical time employed by a single molecule to interact with its molecular neighbors and move around them. Thermal fluctuations (of order $k_B T$) will, in general, spread the set of TS. It is very important to point out that the

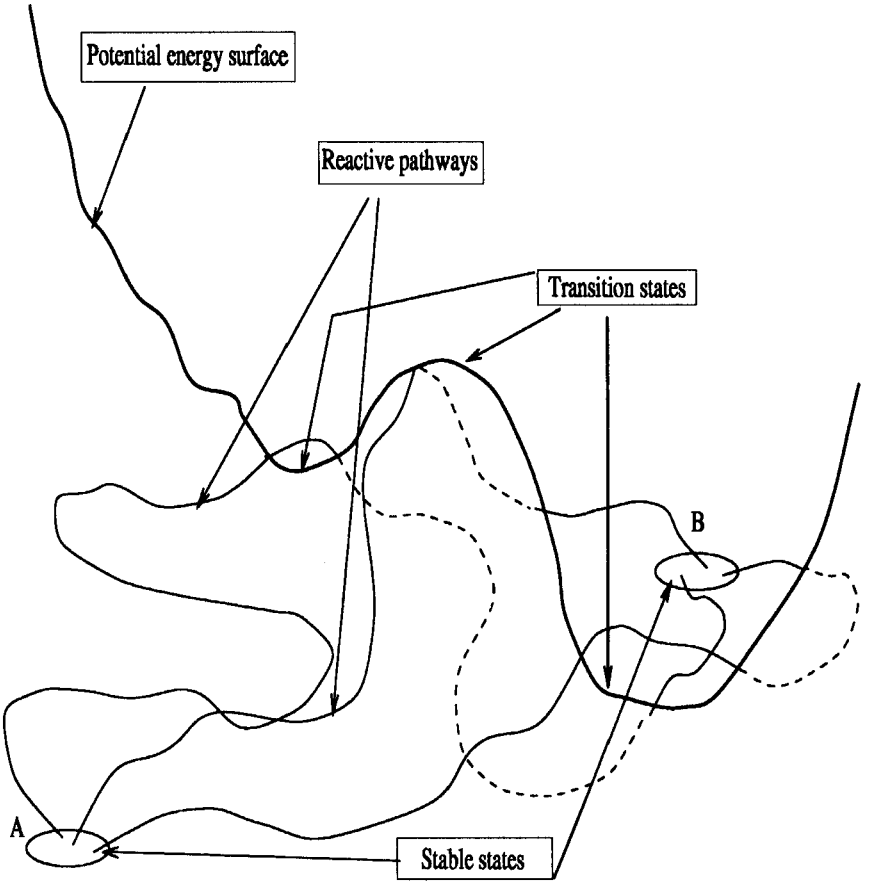

FIGURE 1 Transition paths between two stable states (A, B). The pathways cross the transition states regions located on the potential energy surface.

number of TS visited by the system can be astonishingly large because that number grows exponentially with the dimensionality of the system. The theoretical study of TS is often concerned with calculations involving the location of saddle points on the potential energy surface, as shown in pioneering works by McIver and Komornicki, Cerjan and Miller and others [2, 3]. However, the main drawback of most of the standard methodologies is the use of hypotheses about the exact location of TS. Consequently, a method which does not require *a priori* information about the location of TS is very helpful. An idea pointing to this direction was the use of chains of states between stable regions, as proposed by Pratt [4]. Some researchers have explored this perspective for low dimensional systems in several approximations [5, 6]. A method also based on the suggestions of Pratt is the so-called *transition path sampling*, which has been recently developed [7, 8] in the Newtonian and stochastic versions. The method works by means of the construction of a set of *transition pathways*, which are reactive paths crossing the TS regions in a high dimensional configuration space, in the fashion of Figure 1. Since these paths are associated with a given dynamical process, they will cross the TS region by construction.

Let us apply this technique to a real chemical reaction. We have considered the aqueous dissociation of sodium chloride. The traditional approach to dissociation processes employs the interionic distance, $r_{\text{ion}} = |\mathbf{r}_{Cl^-} - \mathbf{r}_{Na^+}|$ in our case, as the relevant reaction coordinate [9–11]. In this scenario, TS are configurations of the system located on top of the barrier in the potential of mean force, given by the distance $r_{\text{ion}} = r^*_{\text{ion}}$. Nevertheless, that choice of the reaction coordinate leads to a very low value of the transmission coefficient [9]. In this paper, we will assume that the interionic distance is our *order parameter*, i.e. it can serve to distinguish between dissociated and associated configurations in equilibrium. Since this particular order parameter is a poor reaction coordinate and it is only concerned with the solute, we will assume that additional degrees of freedom associated with the solvent will play a relevant role in the dissociation reaction. Several recent works [12–14] have concluded that there is a solvent-related barrier in addition to the ionic potential of mean force. It has been shown that the most important contributions to that barrier are due to nearest neighbor waters to the ion pair. In this paper, we will observe the dynamical evolution of the local structure (up to the second coordination shell) for the system evolving from the associated to the dissociated state paying special attention to the configurations corresponding to the TS of the system.

The computational tool employed has been a stochastic version of the transition path sampling method. We have performed a series of Metropolis Monte Carlo (MC) simulations associated with different time slices. The method works by constructing an ensemble of transition pathways linking two stable states, i.e. those corresponding to the associated and dissociated ion pair. The sampling algorithm to evolve the reactive paths was previously introduced [7]. Once the series of simulations are equilibrated we have located the TS of the system. In previous works, the energetics [13] and the dipole–dipole interactions [14] have been analyzed. Here we focus our attention on the local structure of the solvation process, which has been studied through the calculation of the ion–water partial radial distribution functions, the running coordination numbers and the averaged water populations in the first and second ionic coordination shells.

2. SIMULATION DETAILS

We performed MC simulations of one sodium chloride and $N = 56$ water molecules at the room conditions of $T = 298\,K$ and $\rho = 1.01\,g/cm^3$ ($0.0325\,Å^{-3}$, 1 molal solution) in the NVT ensemble. The waters were modeled with the SPC intermolecular model of Berendsen *et al.* [15], interionic forces were represented with the Huggins-Mayer potential [16] and the ion–water interactions were modeled by Lennard-Jones plus Coulombic terms. We used the same potential parameters employed by Pettitt and Rossky [17] to model interionic and ion–water forces. The system was placed in a cubic box of length $l = 12.062\,Å$ and periodic boundary conditions have been applied. The ionic pair was initially placed along the main diagonal of the box, in order to reduce finite-size effects. In addition, since we will essentially analyze solvation effects on the local ion pair structure, the small sample we are using will not produce important distortions on the correlation functions involved in our study.

Coulombic interactions have been treated using the Ewald summation procedure [18]. We have simulated an ion pair carrying a large dipole moment in molecular water. This fact could produce artificial effects in the simulations and the computed results. Nevertheless, it is important to note that the total charge of the system is zero. As a matter of fact, it has been observed that thermodynamic and structural properties obtained with the Ewald sum rule are totally equivalent to the corresponding results obtained with the reaction field technique, for 5M solutions of NaCl in water and for systems of 250 molecules [19]. Furthermore, detailed calculations of the

ionic-solvation free energies in aqueous NaCl solutions [20] have shown that Ewald summations produce results basically system-size independent for samples of more than 16 water molecules. For those reasons, we will assume the Ewald method is acceptable for our reduced size system.

3. TRANSITION PATH SAMPLING OUTLINE

In order to apply the transition path sampling procedure, we need to define a pair of stable regions located in the configurational space of the system, namely the reactant (state of associated ions) and product (state of dissociated ions) regions (A and B of Fig. 1). We have located those stable regions from the information given by the potential of mean force between the two ions in water, which is defined by

$$\begin{aligned}\Delta W(r_{\text{ion}}) &= W(r_{\text{ion}} + \delta r_{\text{ion}}) - W(r_{\text{ion}}) \\ &= -\frac{1}{\beta} \log \langle \exp\{-\beta \Delta E(r_{\text{ion}})\} \rangle, \end{aligned} \tag{1}$$

where

$$\Delta E(r_{\text{ion}}) = E(r_{\text{ion}} + \delta r_{\text{ion}}) - E(r_{\text{ion}}). \tag{2}$$

Here $\beta = 1/k_B T$ and δr_{ion} is a random trial displacement of the coordinate r_{ion}. We have computed $W(r_{\text{ion}})$ using the perturbative method introduced in Ref. [21]. The calculated potential of mean force $W(r_{\text{ion}})$ is displayed in Figure 2. A dissociation barrier of 2.75 kT is observed around $r^*_{\text{ion}} = 3.8$ Å between two minima located at 2.95 and 4.95 Å. This features are in agreement with other simulation results [22–27]. In summary, we define our reactant region as those configurations which satisfy $r_{\text{ion}} \leq 2.95$ Å and our product region as those configurations with $r_{\text{ion}} \geq 4.95$ Å.

A transition path is assigned to each single particle of the system (atoms and ions). We must keep in mind that only the paths of the two ions are forced to start in the associated state and end up in the dissociated state. The solvating water molecules are not subjected to those constraints. The MC sampling of transition pathways is performed with a path action $S[r_0, \ldots, r_L]$ which weights the set of paths:

$$\begin{aligned}\exp\{-S[r_0, \ldots, r_L]\} &= \mathrm{e}^{-\beta E(r_0)} h_A[r_{\text{ion}}(\tau = 0)] \\ &\quad \times \left(\prod_{\tau=0}^{L-1} p[r_\tau \rightarrow r_{\tau+1}] \right) h_B[r_{\text{ion}}(\tau = L)]. \end{aligned} \tag{3}$$

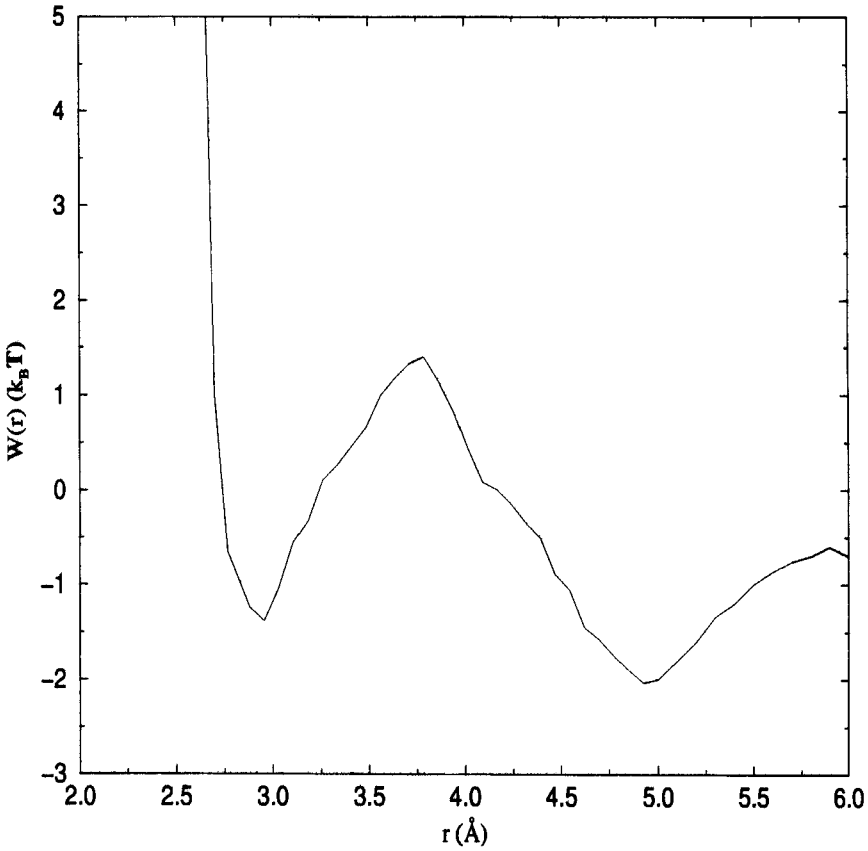

FIGURE 2 Potential of mean force $W(r_{\text{ion}})$ between sodium and chlorine in water. The cumulative error is 0.05 k_BT.

Here τ is the time label ($\tau = 0, \ldots, L = 150$), r_τ is a point in configurational space, $p[r_\tau \rightarrow r_{\tau+1}]$ is the conditional probability of an atom to visit the configuration $r_{\tau+1}$ provided it was in r_τ in time τ and $E(r_\tau)$ is the potential energy of the configuration r_τ. Each time label is called a *time slice* and the time interval $\Delta\tau$ between two consecutive time slices is defined as 1. The number of time slices L has been chosen according the following rule: it is the value which allows a realistic simulation length with the lowest computational cost. This cost is approximately proportional to L. In our case, it has been found (see discussion in Ref. [13]) that the time length of our MC simulations is longer than 1 ps, which is sufficient to monitor the sodium chloride dissociation. The boundaries for the ion pair are given by

$h_A[r_{\text{ion}}(\tau = 0)]$ and $h_B[r_{\text{ion}}(\tau = L)]$:

$$h_A[r_{\text{ion}}(\tau = 0)] = \begin{cases} 1, & r_{\text{ion}} \leq 2.95\,\text{Å} \\ 0, & \text{otherwise.} \end{cases}$$

$$h_B[r_{\text{ion}}(\tau = L)] = \begin{cases} 1, & r_{\text{ion}} \geq 4.95\,\text{Å} \\ 0, & \text{otherwise.} \end{cases} \tag{4}$$

The transition probability $p[r_\tau \to r_{\tau+1}]$ is a normalized Markovian probability which conserves the Boltzmann distribution and satisfies detailed balance. In this work, we employed:

$$p(r_\tau \to r'_\tau) = w(r_\tau \to r'_\tau) + \delta(r_\tau - r'_\tau)Q(r_\tau), \tag{5}$$

where the transition probability for an accepted MC trial $w(r_\tau \to r'_\tau)$ and the rejection probability $Q(r_\tau)$ are, respectively:

$$w(r_\tau \to r'_\tau) = \eta(r_\tau, r'_\tau) \min\left[1, e^{-\beta(E(r'_\tau)-E(r_\tau))}\right]$$
$$Q(r_\tau) = 1 - \int dr''_\tau\, w(r_\tau \to r''_\tau). \tag{6}$$

The functions $\eta(r_\tau, r'_\tau)$ have been chosen as products of Gaussians with variances $\sigma_T = 0.25$ Å (translations) and $\sigma_R = 0.35$ rad (rotations). We sampled the action (3) with the so-called *shooting* algorithm (see Ref. [8]). The shooting algorithm works by randomly picking a time slice along the transition path and re-growing the entire path forward and backward in time. The acceptance probability of a shooting trial is equal to the characteristic function (4) of the target boundary, i.e. every trial which satisfies the boundary constraint is accepted:

$$P_{\text{acc.}}^{\text{forward}}\,(r_0, \ldots, r_\tau, r'_{\tau+1}, \ldots, r'_L) = h_B[r'_{\text{ion}}(\tau = L)],$$
$$P_{\text{acc.}}^{\text{backward}}(r'_0, \ldots, r'_{\tau-1}, r_\tau, \ldots, r_L) = h_A[r'_{\text{ion}}(\tau = 0)]. \tag{7}$$

The tools described above allowed us the preparation of an ensemble of transition paths. The second part of the method concerns the location of TS which will correspond, in the framework of the theory, to maxima of the transition paths. We need a method useful to identify the extremal points of each transition pathway. Once TS are located, we will generate a set of realizations of the TS, which we call the *TS ensemble* [28]. To calculate the TS ensemble we use an *equal probability* criterion: a configuration r_τ is a TS of the system if trial trajectories of length L starting at r_τ have an equal

probability of 0.5 to reach both endpoints [29]. Trial trajectories are generated at random starting at r_τ by means of the shooting algorithm. In practice we employ 50 trials for each time slice and count the number of successful trajectories started at r_τ which end up in each stable state. This is a very expensive calculation since we need to construct *auxiliary* trajectories for each of the L time slices of a path. Therefore, when the number of auxiliary paths ending at each stable region is approximately equal, the configuration r_τ is considered a member of the TS ensemble. Finally, the transition pathways need to be relabeled in order to match the TS at the same time slice for each path: we assign $\tau = 0$ to the TS. This solves the alignment problem caused by the realization of the TS at different time slices for each path. The number of time slices for each path is now lower than L: only those labels common to all reactive paths survive [13, 14].

4. DISCUSSION

An equilibration run of 12000 MC passes for each time slice has been performed prior to collecting significant data. We have harvested and located the corresponding TS of 350 paths. The acceptance rate for transition paths was 11%.

To observe the evolution of the local solvent structure around the ion pair we display a set of three selected snapshots [30] in Figures 3 (associated ions), 4 (transition state) and 5 (dissociated ions). We can note that the ion pair suffers significant changes during dissociation, as well as both the first and second ionic coordination shells. The first coordination shells are defined as spheres centered at the ionic positions and of radius $R_{Na^+} = 3.25$ Å and $R_{Cl^-} = 4$ Å. The second coordination shells have been defined as spherical layers of internal radius of 3.25 Å for sodium and 4 Å for chlorine and external radius of 5 Å for sodium and 5.5 Å for chlorine.

The ion pair is separated apart by solvating waters during dissociation. In the associated state, first coordination shell waters are observed to be close to the solute, whereas they slightly spread their positions in the TS and dissociated configurations. The most significant feature is the incoming two waters (in average) which take a place in between the ion pair and stablish themselves as a "bridge" between the two ions in the TS configuration. Similar graphical information was already reported from molecular dynamics calculations [24]. We will address again this point when discussing ionic coordination numbers. These waters will clearly come from the second coordination shell. Concerning the second shell, we note an increase of its

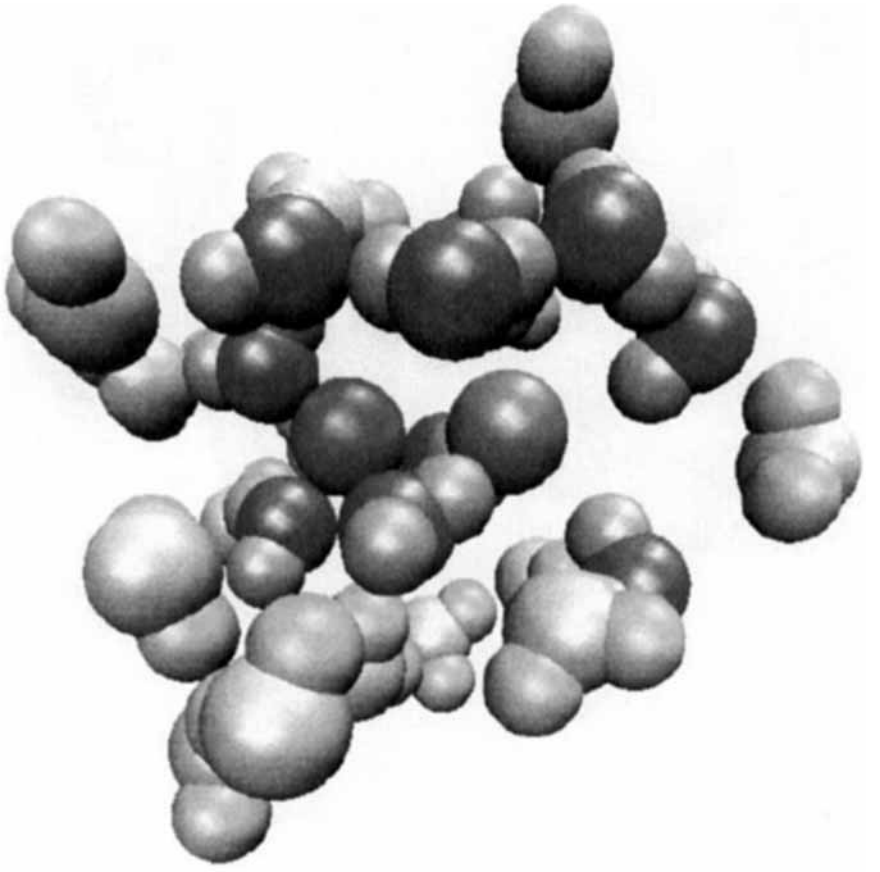

FIGURE 3 Snapshot of a typical configuration in the state of associated ions. Sodium is depicted in red, chlorine in green, oxygens and hydrogens of the first coordination shell are depicted in blue and orange, respectively. Oxygens and hydrogens of the second coordination shell are depicted in iceblue and yellow, respectively. (See Color Plate I).

population during the dissociation process. The spatial distribution of second shell waters tends to create voids to allocate the ion pair, as we will show below.

The partial ion–oxygen and ion–hydrogen radial distribution functions $g(r)$ are given by

$$g(r) = \frac{V}{N}\frac{n(r)}{4\pi r^2 \Delta r} \tag{8}$$

where $V = l^3$ and $n(r)$ is the number of waters inside a spherical layer of thickness Δr and radius r centered at the ion. We show $g_{ONa}(r)$ and $g_{OCl}(r)$

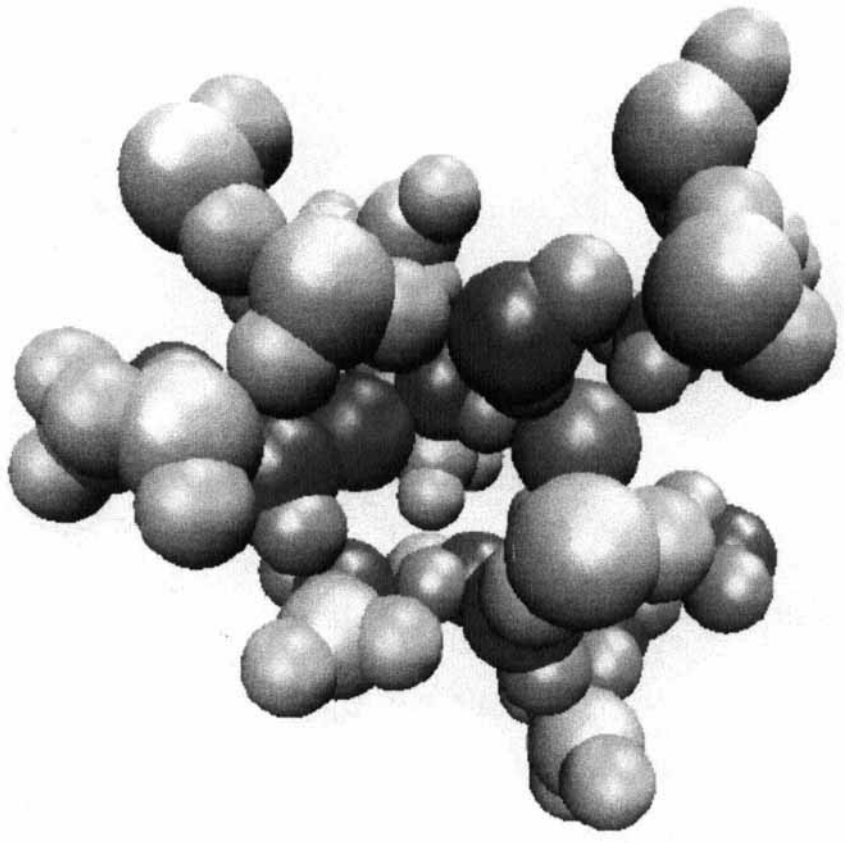

FIGURE 4 Snapshot of a typical configuration of the TS ensemble. Colors are the same as used in Figure 3. (See Color Plate II).

in Figure 6 and $g_{HNa}(r)$ and $g_{HCl}(r)$ in Figure 7. We report a comparison between the dissociated state and the TS. The first peak of all radial distribution functions is basically equivalent for the two types of configurations. Relevant differences appear in the maxima due to the second ionic coordination shells: we note in all cases a shift to higher values of the bands corresponding to TS configurations when comparing with configurations of the state with dissociated ions. This effect is especially clear in the sodium case. We can explain those features in the following way: the first coordination shells are strongly related to typical ion–water distances produced by direct interactions, i.e. the first shell peaks are located at the positions determined by the sizes of water and ions (Lennard-Jones) as well as by the electrostatic (Coulomb) forces. Conversely, the second shell

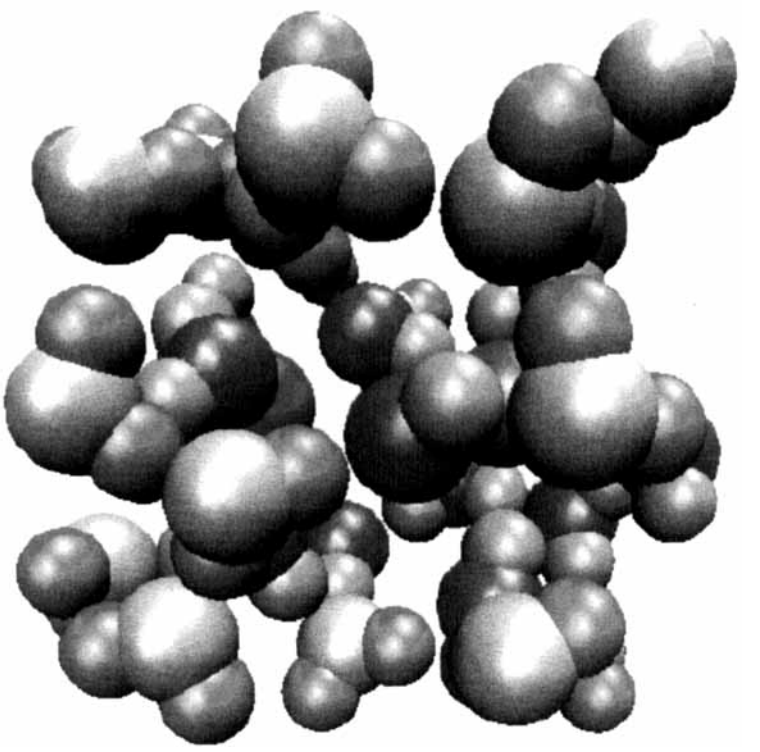

FIGURE 5 Snapshot of a typical configuration in the state of dissociated ions. Colors are the same as used in Figures 3 and 4. (See Color Plate III).

has to deal with water–water interactions and with the dissociation process which is happening inside. The bigger size associated to the second coordination shell in the TS ensemble indicates that waters are creating a free space to allocate the ion pair after dissociation. Later on, the water–ion distance is reduced again in the state of dissociated ions.

Once the radial distributions functions have been obtained, we have computed the corresponding averaged coordination numbers $n(r)$:

$$n(r) = 4\pi\rho \int_0^r dr' r'^2 g(r'). \tag{9}$$

The results for the oxygen–sodium and hydrogen–chlorine coordination numbers are displayed in Figure 8. We have only reported those two functions because they correspond to the $g(r)$ which have a good asymptotical behavior. The reader should note that, because of the small size of our simulation box, we can report the $g(r)$ only until a distance of

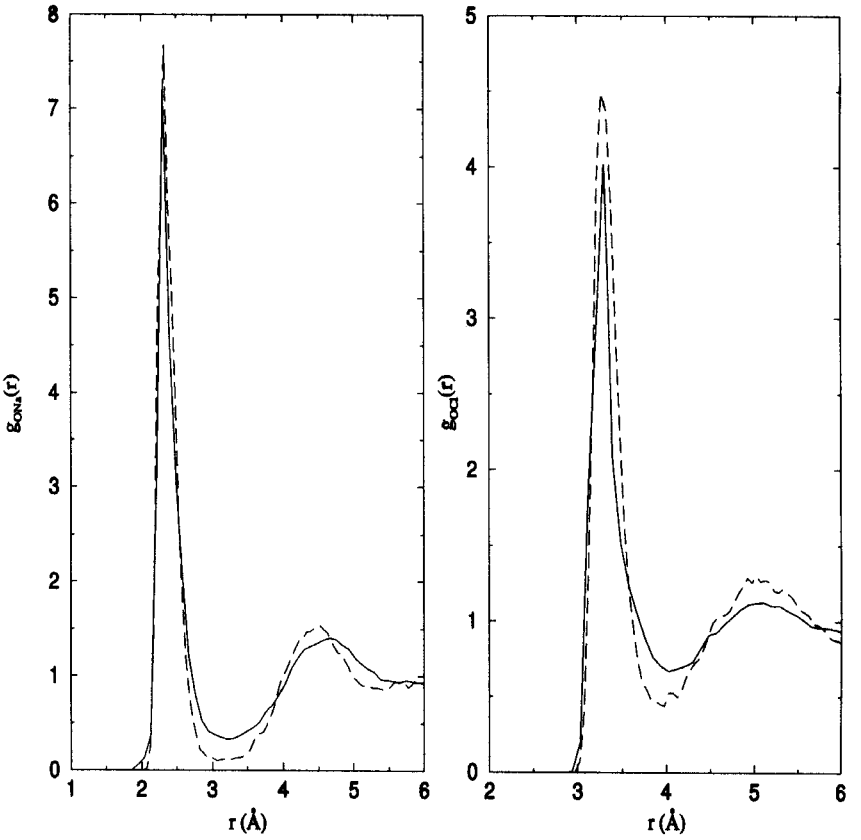

FIGURE 6 Radial oxygen–ion distribution functions: comparison between configurations corresponding to the TS ensemble (full line) and to the state of dissociated ions (dashed line).

$r = 6$ Å. We must point out that $n_{HCl}(r)$ has been computed as the mean number of waters (instead of hydrogens) in the first chlorine shell. We report again a comparison between the dissociated state and the ensemble of configurations at the TS of the system. In order to complete this partial results, we have counted and averaged the populations of oxygens corresponding to first and second ionic coordination shells for TS and stable states. The results and experimental data available are reported in Table I. To compare these results with the snapshots displayed in Figures 3–5, we should remember that the coordination shells of each ion are defined to have some common volume and consequently, a few waters can pertain simultaneously to both sodium and chlorine shells.

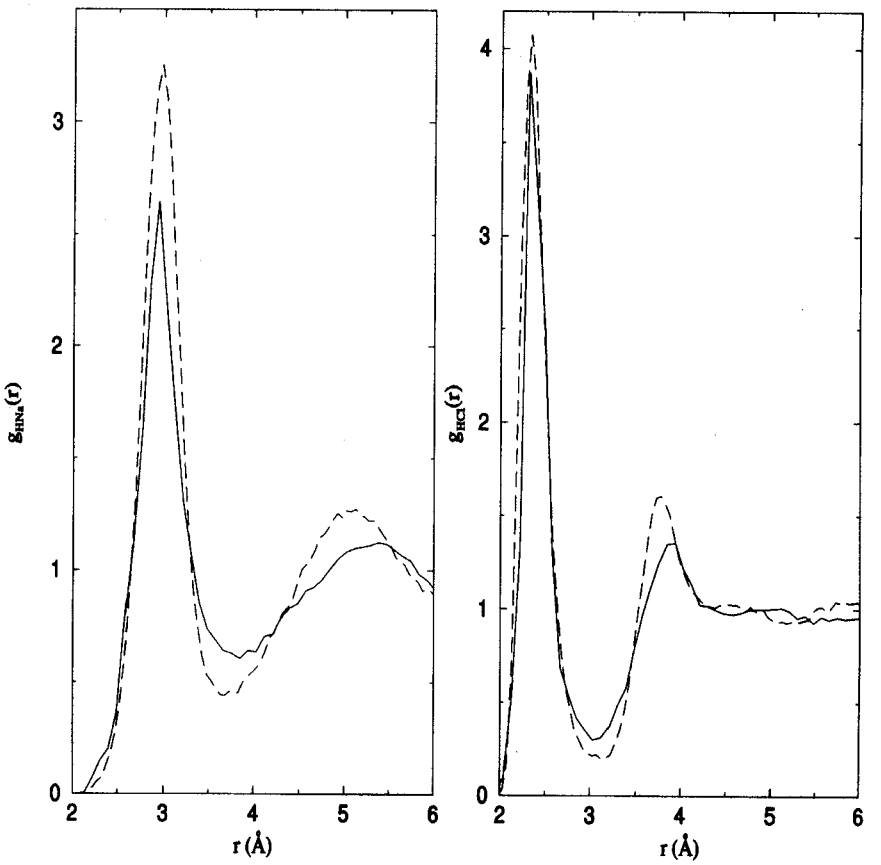

FIGURE 7 Radial hydrogen-ion distribution functions using same symbols as in Figure 6.

The shape of the partial $n_{ONa}(r)$ for TS and the state with dissociated ions is remarkably different, whereas there is a greater similarity for the $n_{HCl}(r)$. Essentially, the number of neighboring waters for each of the two ions after dissociation is larger than in the TS ensemble. Those results are confirmed by the data of Table I. The increase of $n(r)$ for sodium during the dissociation process is about two waters, whereas the population of the chlorine first shell grows (in average) in one water unit during dissociation. We note that the solvation of the ion pair is basically due to a few additional waters which are provided by the second coordination shell. There is good agreement between our results and experimental data available [31, 32] measured from neutron diffraction and X-ray scattering measurements. The

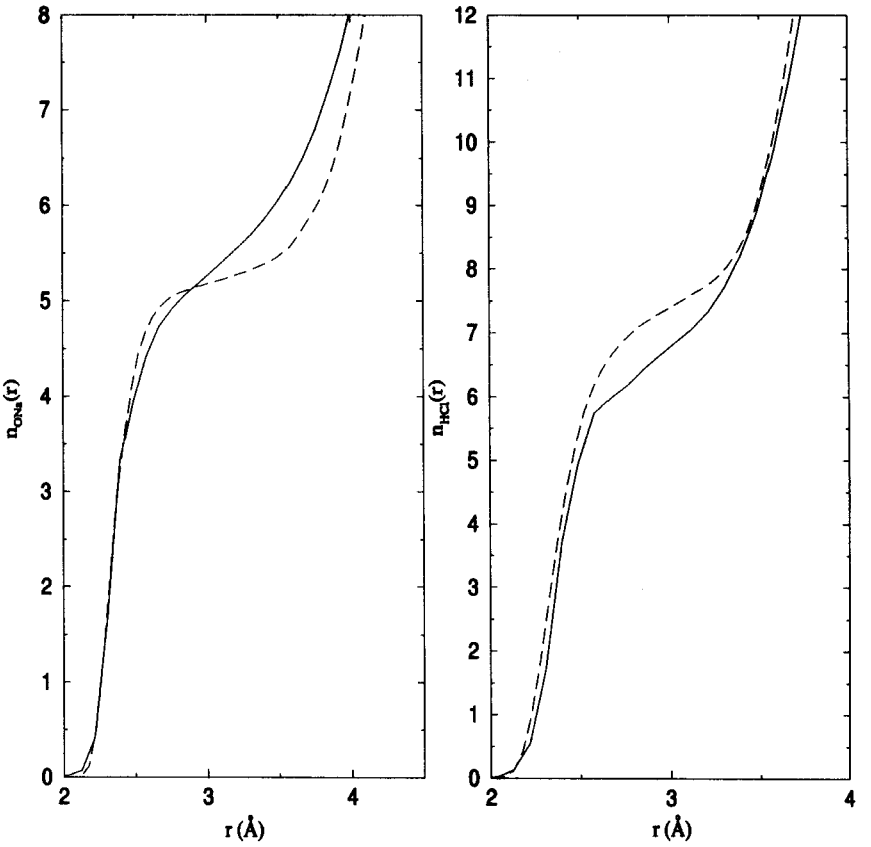

FIGURE 8 Running coordination numbers $n_{ONa}(r)$ and $n_{HCl}(r)$. TS ensemble (full line) and the dissociated ions (dashed line).

TABLE I Coordination numbers and water populations for TS and the stable states. The error estimate is about 0.3 for all the simulated values

	$n_{Na^+O}(r)$		$n_{Cl^-O}(r)$	
	First shell	*Second shell*	*First shell*	*Second shell*
Associated	4.3	5.2	6.3	13.4
TS	5.7	6.8	7.0	14.2
Dissociated	6.1	8.9	7.6	14.4
Experimental	4 – 6 [31]	–	6.4 ± 0.3 [32]	–

populations of the second coordination shells are basically stable for chlorine whereas we observe an increase of two waters in the sodium shell during dissociation.

5. CONCLUDING REMARKS

The transition path sampling methodology has been applied in a stochastic version to the study of the dynamics of the local structure in the dissociation of sodium chloride in water. We have used the potential of mean force $W(r_{ion})$ to locate the two stable regions (reactants and products of the reaction) linked by transition paths, composed by a finite number of time slices. We have generated an equilibrated ensemble of reactive pathways by means of the path action and of the shooting algorithm. The location of the TS has been done using an equal probability criterion: a time slice is a member of the TS ensemble if the probability of ending up by shooting on each of the stable states is approximately 0.5.

We analyzed the structural features of the Na–Cl dissociation paying attention to the ion–water radial distribution functions, to the corresponding coordination numbers as well as to the first and second ionic shell water populations (Tab. I). First, we observed the computed water populations in the first ionic shells are in good agreement with experimental data. Secondly, it has been noted the addition of two waters (on average) to the sodium first shell and of one water to the chlorine first shell along the dissociation process. Finally, the partial radial distribution functions show that ionic second solvation shells are slightly displaced to larger values in the TS ensemble which indicates that, in order to provide the room for the ion pair after dissociation waters in the second shell produce temporal voids. We conclude that the reorganization of the solvent by means of the two processes described above is the main responsible for the sodium-chloride dissociation.

Acknowledgements

The author is indebted to Dr. Felix Csajka and Prof. David Chandler for their permanent support and for fruitful discussions and suggestions. I am also grateful to the Direcció General de Recerca of the Generalitat de Catalunya, which provided the post-doctoral grant 1995BEAI300020 of the CIRIT program and the project 1997SGR-00149 as well as to the Ministerio de Educación y Ciencia of Spain, project PB96-0170-C03-02. Project PR99-05 of the Polytechnical University of Catalonia and funds from the National Science Foundation and the US Department of Energy through the Chemical Sciences Division of the Lawrence Berkeley National Laboratory have partially supported this work and are also acknowledged.

References

[1] Hänggi, P., Talkner, P. and Borkovec, M. (1990). "Reaction-rate theory: fifty years after Kramers", *Rev. Mod. Phys.*, **62**, 251.

[2] McIver, J. and Komornicki, A. (1972). "Structure of transition states in organic reactions. General theory and an application to cyclobutene-butadiene isomerization using a semiempirical molecular orbital method", *J. Am. Chem. Soc.*, **94**, 2625.

[3] Cerjan, C. J. and Miller, W. H. (1981). "On finding transition states", *J. Chem. Phys.*, **75**, 2800.

[4] Pratt, L. R. (1986). "A statistical method for identifying transition states in high dimensional problems", *J. Chem. Phys.*, **85**, 5045.

[5] Choi, C. and Elber, R. (1991). "Reaction path study of helix formation in tetrapeptides: Effect of side chains", *J. Chem. Phys.*, **94**, 751.

[6] Sevick, E. M., Bell, A. T. and Theodorou, D. N. (1993). "A chain of states method for investigating infrequent event processes in multistate, multidimensional systems", *J. Chem. Phys.*, **98**, 3196.

[7] Dellago, C., Bolhuis, P. G., Csajka, F. S. and Chandler, D. (1998). "Transition path sampling and the calculation of rate constants", *J. Chem. Phys.*, **108**, 1964.

[8] Dellago, C., Bolhuis, P. G. and Chandler, D. (1999). "On the calculation of reaction rate constants in the transition path ensemble", *J. Chem. Phys.*, **110**, 6617.

[9] Karim, O. A. and McCammon, J. A. (1986). "Rate constants for ion pair formation and dissociation in water", *Chem. Phys. Lett.*, **132**, 219.

[10] Rey, R. and Guárdia, E. (1992). "Dynamical aspects of the $Nat^+ - Cl^-$ ion pair association in water", *J. Phys. Chem.*, **96**, 4712.

[11] Rey, R., Guàrdia, E. and Padró, J. A. (1992). "Generalized Langevin dynamics simulation of activated processes in solution: Ion pair interconversion in water", *J. Chem. Phys.*, **97**, 8276.

[12] Geissler, P. L., Dellago, C. and Chandler, D. (1999). "Kinetic pathways of ion pair dissociation in water", *J. Phys. Chem. B*, **103**, 3706.

[13] Martí, J. and Csajka, F. S. (2000). "The aqueous solvation of sodium chloride: A Monte Carlo transition path sampling study", *J. Chem. Phys.*, **113**, 1154.

[14] Martí, J., Csajka, F. S. and Chandler, D. (2000). "Stochastic transition pathways in the aqueous sodium chloride dissociation process", *Chem. Phys. Lett.*, **328**, 169.

[15] Berendsen, H. J. C., Postma, J. P. M., van Gunsteren, M. F. and Hermans, J., "Interaction models for water in relation to protein hydration", In: *Intermolecular forces*, Pullman, B. Ed., Reidel, Dordretch, Holland, 1981, pp. 331–342.

[16] Huggins, M. L. and Mayer, J. E. (1933). "Interatomic distances in crystals of the alkali halides", *J. Chem. Phys.*, **1**, 643.

[17] Pettitt, B. M. and Rossky, P. J. (1986). "Alkali halides in water: Ion–solvent correlations and ion–ion potentials of mean force at infinite dilution", *J. Chem. Phys.*, **84**, 5836.

[18] Allen, M. P. and Tildesley, D. J. (1987). "*Computer Simulation of Liquids*", Clarendon, Oxford.

[19] Hummer, G., Soumpasis, D. M. and Neumann, M. (1994). "Computer simulations do not support Cl–Cl pairing in aqueous NaCl solution", *Mol. Phys.*, **81**, 1155.

[20] Hummer, G., Pratt, L. R. and García, A. E. (1997). "Ion sizes and finite-size corrections for ionic-solvation free energies", *J. Chem. Phys.* **107**, 9275.

[21] Voter, A. F. (1985). "A Monte Carlo method for determining free-energy differences and transition state theory rate constants", *J. Chem. Phys.*, **82**, 1890.

[22] Berkowitz, M., Karim, O. A., McCammon, J. A. and Rossky, P. J. (1984). "Sodium chloride ion pair interaction in water: computer simulation", *Chem. Phys. Lett.*, **105**, 577.

[23] Dang, L. X., Rice, J. E. and Kollman, P. A. (1990). "The effect of water models on the interaction of the sodium-chloride ion pair in water: Molecular dynamics simulations", *J. Chem. Phys.*, **93**, 7528.

[24] Guárdia, E., Rey, R. and Padró, J. A. (1991). "Potential of mean force by constrained molecular dynamics: a sodium chloride ion-pair in water", *Chem. Phys.*, **155**, 187.

[25] Smith, D. E. and Haymet, A. D. J. (1992). "Structure and dynamics of water and aqueous solutions: The role of flexibility", *J. Chem. Phys.*, **96**, 8450.

[26] Smith, D. E. and Dang, L. X. (1994). "Computer simulations of NaCl association in polarizable water", *J. Chem. Phys.*, **100**, 3757.
[27] Friedman, R. A. and Mezei, M. (1995). "The potentials of mean force of sodium chloride and sodium dimethylphosphate in water: An application of adaptative umbrella sampling", *J. Chem. Phys.*, **102**, 419.
[28] Bolhuis, P. G., Dellago, C. and Chandler, D. (1998). "Sampling ensembles of deterministic transition pathways", *Faraday Discussion Chem. Soc.*, **110**, 421.
[29] Du, R., Pande, V. S., Grosberg, A. Y., Tanaka, T. and Shakhnovich, E. (1998). "On the transition coordinate for protein folding", *J. Chem. Phys.*, **108**, 334.
[30] Humphrey, W., Dalke, A. and Schulten, K. (1996). "VMD-Visual Molecular-Dynamics", *J. Molec. Graphics*, **14**, 33.
[31] Neilson, G. W. and Enderby, J. E. (1979). "Neutron and X-ray diffraction studies of concentrated aqueous electrolyte solutions", *Annu. Rep. Prog. Chem.*, **C76**, 185.
[32] Powell, D. H., Neilson, G. W. and Enderby, J. E. (1993). "The structure of Cl^- in aqueous solution: An experimental determination of $g_{ClH}(r)$ and $g_{ClO}(r)$", *J. Phys. Condens. Matter*, **5**, 5723.